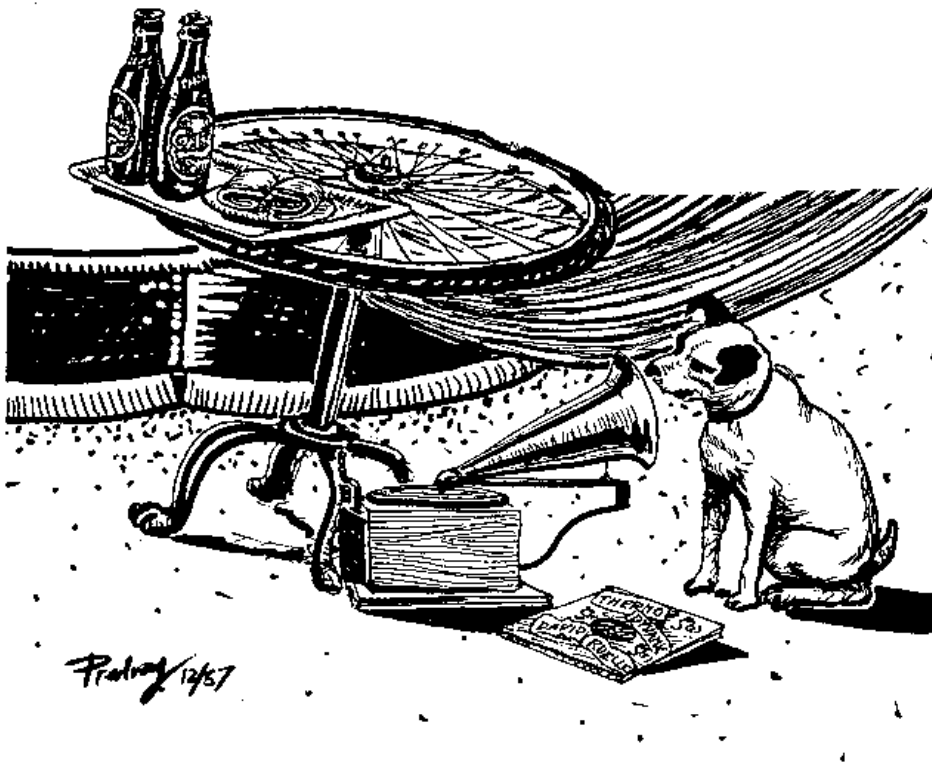


Chaos: Classical and Quantum

I: Deterministic Chaos



Predrag Cvitanović – Roberto Artuso – Ronnie Mainieri – Gregor Tanner –
Gábor Vattay

Chapter 31

Universality in transitions to chaos

When you come to a fork in the road, take it!
—Yogi Berra

THE DEVELOPMENTS that we shall describe next are one of those pleasing demonstrations of the unity of physics. The key discovery was made by a physicist not trained to work on problems of turbulence. In the fall of 1975 Mitchell J. Feigenbaum, an elementary particle theorist, discovered a universal transition to chaos in 1-dimensional unimodal map dynamics. At the time the physical implications of the discovery were nil. During the next few years, however, numerical and mathematical studies established this universality in a number of realistic models in various physical settings, and in 1980 the universality theory passed its first experimental test.

The discovery was that large classes of nonlinear systems exhibit transitions to chaos which are *universal* and *quantitatively* measurable. This advance was akin to (and inspired by) earlier advances in the theory of phase transitions; for the first time one could, predict and measure ‘critical exponents’ for turbulence. But the breakthrough consisted not so much in discovering a new set of universal numbers, as in developing a new way to solve strongly nonlinear physical problems. Traditionally, we use regular motions (harmonic oscillators, plane waves, free particles, etc.) as zeroth-order approximations to physical systems, and account for weak nonlinearities perturbational. We think of a dynamical system as a smooth system whose evolution we can follow by integrating a set of differential equations. The universality theory tells us that the zeroth-order approximations to strongly nonlinear systems should be quite different. They show an amazingly rich structure which is not at all apparent in their formulation in terms of differential equations; instead, they exhibit self-similar structures which can be encoded by universality equations of a type which we will describe here. To put it more provocatively: junk your old equations and look for guidance in clouds’ repeating patterns.

Figure 31.1:

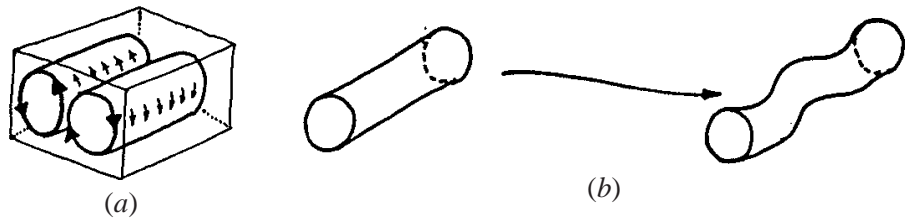
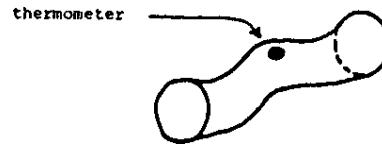


Figure 31.2



In this chapter we reverse the chronology, describing first a turbulence experiment, then a numerical experiment, and finally explain the observations using the universality theory. We will try to be intuitive and concentrate on a few key ideas. Even though we illustrate it by onset of turbulence, the universality theory is by no means restricted to the problems of fluid dynamics.

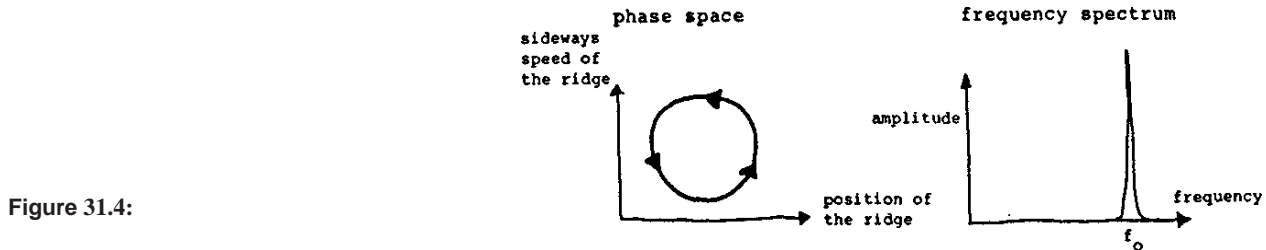
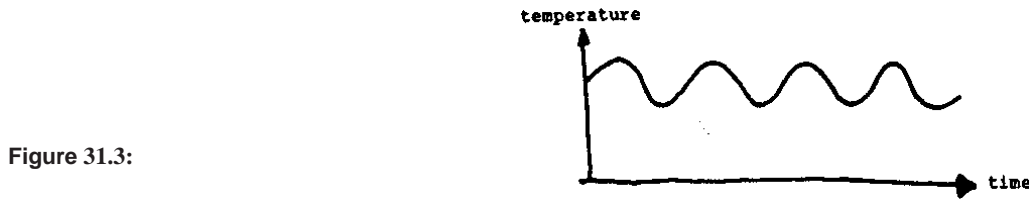
31.1 Onset of turbulence

We start by describing schematically the 1980 experiment of Libchaber and Maurer. In the experiment a liquid is contained in a small box heated from the bottom. The salient points are:

1. There is a *controllable parameter*, the Rayleigh number, which is proportional to the temperature difference between the bottom and the top of the cell.
2. The system is *dissipative*. Whenever the Rayleigh number is increased, one waits for the *transients to die out*.
3. The container, figure 31.1 (a), has a small “aspect ratio”; its width is a small integer multiple of its height, approximately.

For small temperature gradients there is a heat flow across the cell, but the liquid is static. At a critical temperature a convective flow sets in. The hot liquid rises in the middle, the cool liquid flows down at the sides, and two convective rolls appear. So far everything is as expected from standard bifurcation scenarios. As the temperature difference is increased further, the rolls become unstable in a very specific way - a wave starts running along the roll, figure 31.1 (b), figure 31.1 (b).

As warm liquid is rising on one side of the roll, cool liquid is descending down the other side, the position and the sideways velocity of the ridge can be measured with a thermometer, figure 31.2. One observes a sinusoid, figure 31.3. The periodicity of this instability suggests two other ways of displaying the measurement, figure 31.4.



Now the temperature difference is increased further. After the stabilization of the state space trajectory, a new wave is observed superimposed on the original sinusoidal instability. The three ways of looking at it (real time, state space, frequency spectrum) are sketched in figure 31.5. A coarse measurement would make us believe that T_0 is the periodicity. However, a closer look reveals that the state space trajectory misses the starting point at T_0 , and closes on itself only after $2T_0$. If we look at the frequency spectrum, a new wave band has appeared at half the original frequency. Its amplitude is small, because the state space trajectory is still approximately a circle with periodicity T_0 .

As one increases the temperature very slightly, a fascinating thing happens: the state space trajectory undergoes a very fine splitting, see figure 31.6. We see that there are three scales involved here. Looking casually, we see a circle with period T_0 ; looking a little closer, we see a pretzel of period $2T_0$; and looking very closely, we see that the trajectory closes on itself only after $4T_0$. The same information can be read off the frequency spectrum; the dominant frequency is f_0 (the circle), then $f_0/2$ (the pretzel), and finally, much weaker $f_0/4$ and $3f_0/4$.

The experiment now becomes very difficult. A minute increase in the temperature gradient causes the state space trajectory to split on an even finer scale, with the periodicity $2^3 T_0$. If the noise were not killing us, we would expect these splittings to continue, yielding a trajectory with finer and finer detail, and a frequency spectrum of figure 31.7, with families of ever weaker frequency components. For a critical value of the Rayleigh number, the periodicity of the system is $2^\infty T_0$, and the convective rolls have become turbulent. This *weak turbulence* is today usually referred to as the ‘onset of chaos’. Globally, the rolls persist but are wiggling irregularly. The ripples which are running along them show no periodicity, and the spectrum of an idealized, noise-free experiment contains infinitely many subharmonics, figure 31.8. If one increases the temperature gradient beyond this critical value, there are further surprises (see, for example, figure 31.16) which we will not discuss here.

We now turn to a numerical simulation of a simple nonlinear oscillator in order to start understanding why the state space trajectory splits in this peculiar fashion.

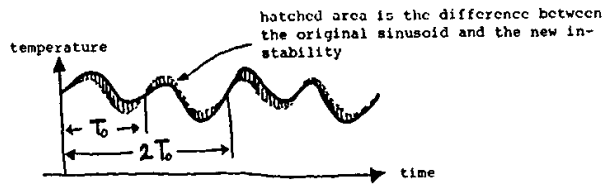


Figure 31.5:

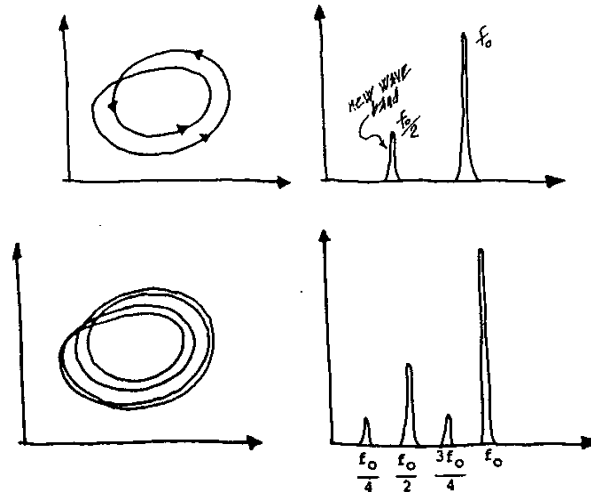


Figure 31.6:

31.2 Onset of chaos in a numerical experiment

In the experiment that we have just described, limited experimental resolution makes it impossible to observe more than a few bifurcations. Much longer sequences can be measured in numerical experiments. A typical example is the nonlinear oscillator

exercise 31.2

$$\ddot{x} + \gamma\dot{x} - x + 4x^3 = A \cos(\omega t). \tag{31.1}$$

The oscillator is driven by an external force of frequency ω , with amplitude A period $T_0 = 2\pi/\omega$. The dissipation is controlled by the friction coefficient γ . (See (2.21) and example 8.1.) Given the initial displacement and velocity one can easily follow numerically the state space trajectory of the system. Due to the dissipation it does not matter where one starts; for a wide range of initial points the state space trajectory converges to an attracting *limit cycle* (trajectory loops onto itself) which for some $\gamma = \gamma_0$ looks something like figure 31.9. If it were not for the external driving force, the oscillator would have simply come to a stop. As it is, executing a motion forced on it externally, independent of the initial displacement and velocity. Starting at the point marked 1, the pendulum returns to it after the unit period T_0 .

However, as one decreases, the same phenomenon is observed as in the turbulence experiment; the limit cycle undergoes a series of period-doublings, figure 31.10. The trajectory keeps on nearly missing the starting point, until it hits after exactly $2^n T_0$. The state space trajectory is getting increasingly hard to draw; however, the sequence of points 1, 2, ..., 2^n , which corresponds to the state of the oscillator at times $T_0, 2T_0, \dots, 2^n T_0$, sits in a small region of the state space, so in figure 31.11 we enlarge it for a closer look. Globally the trajectories of the

Figure 31.7:

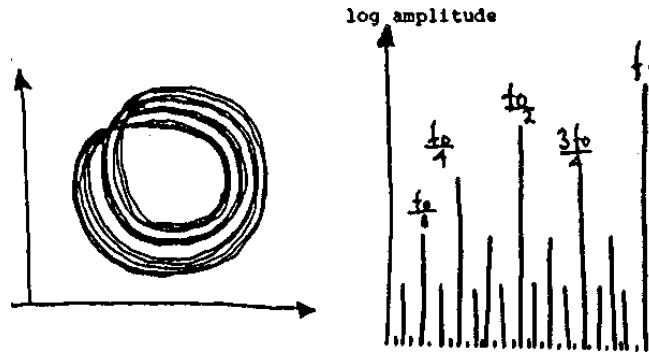


Figure 31.8:



turbulence experiment and of the non-linear oscillator numerical experiment look very different. However, the above sequence of near misses is *local*, and looks roughly the same for both systems. This sequence of points lies approximately on a straight line, figure 31.12. Let us concentrate on this line, reducing the dimensionality of the state space by a Poincaré map. The Poincaré map contains all the information we need; from it we can read off when an instability occurs, and how large it is. One varies continuously the non-linearity parameter (friction, Rayleigh number, etc.) and plots the location of the intersection points; in the present case, the Poincaré surface is - for all practical purposes - a smooth 1-dimensional curve, and the result is a *bifurcation tree* of figure 31.13. We already have some *qualitative* understanding of this plot. The state space trajectories we have drawn are localized (the energy of the oscillator is bounded) so the tree has a finite span. Bifurcations occur simultaneously because we are cutting a single trajectory; when it splits, it does so everywhere along its length. Finer and finer scales characterize both the branch separations and the branch lengths.

Feigenbaum's discovery consists of the following *quantitative* observations:

1. The *parameter convergence* is universal (i.e., independent of the particular physical system), $\Delta_i/\Delta_{i+1} \rightarrow 4.6692\dots$ for i large, see figure 31.14.
2. The relative scale of successive *branch splittings* is universal: $\epsilon_i/\epsilon_{i+1} \rightarrow 2.5029\dots$ for i large, see figure 31.15.

The beauty of this discovery is that if turbulence (chaos) is arrived at through an infinite sequence of bifurcations, we have two quantitative predictions:

1. The convergence of the critical Rayleigh numbers corresponding to the cycles of length 2, 4, 8, 16, ... is controlled by the universal convergence parameter $\delta = 4.6692016\dots$

Figure 31.9:

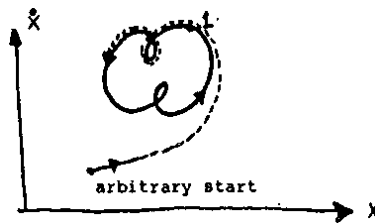
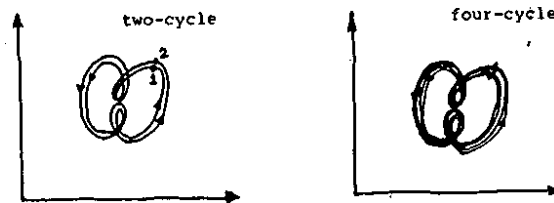


Figure 31.10:



2. The splitting of the state space trajectory is controlled by the universal scaling parameter $\alpha = 2.50290787 \dots$. As we have indicated in our discussion of the turbulence experiment, the relative heights of successive subharmonics measure this splitting and hence α .

While this universality was derived through study of simple, few-dimensional systems (pendulum, oscillations along a convective roll), it also applies to high- or even infinite-dimensional systems, such as discretizations of the Navier-Stokes equations, and in the literature there are innumerable other examples of period-doublings in many-dimensional systems. A wonderful thing about this universality is that it does not matter much how close our equations are to the ones chosen by nature; as long as the model is in the same universality class (in practice this means that it can be modeled by a mapping of form (31.2)) as the real system, both will undergo a period-doubling sequence. That means that we can get the right physics out of very simple models, and this is precisely what we will do next.

Example 31.1 Period doubling tree in a flame flutter. For $\nu > 1$, $u(x, t) = 0$ is the globally attractive stable equilibrium; starting with $\nu = 1$ the solutions go through a rich sequence of bifurcations.

Figure 31.16 is a representative plot of the period-doubling tree for the Poincaré map P . To obtain this figure, we took a random initial point, iterated it for a some time to let it settle on the attractor and then plotted the a_6 coordinate of the next 1000 intersections with the Poincaré section. Repeating this for different values of the damping parameter ν , one can obtain a picture of the attractor as a function of ν ; the dynamics exhibits a rich variety of behaviors, such as strange attractors, stable limit cycles, and so on.

The reason why multidimensional *dissipative* systems become effectively 1-dimensional is that: for dissipative systems state space volumes shrink. They shrink at different rates in different directions, as in figure 31.17. The direction of the slowest convergence defines a 1-dimensional line which will contain the attractor (the region of the state space to which the trajectory is confined at asymptotic times)

Figure 31.11:

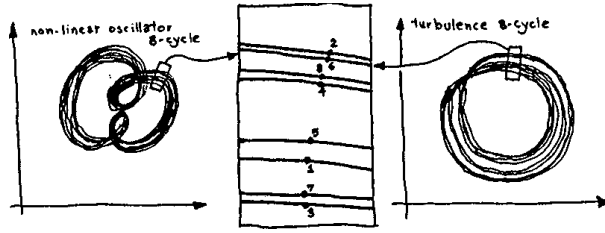
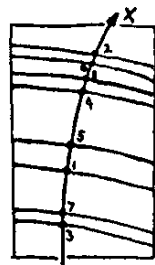


Figure 31.12:



What we have presented so far are a few experimental facts; we now have to convince you that they are universal.

31.3 What does all this have to do with fishing?

Looking at the state space trajectories shown earlier, we observe that the trajectory bounces within a restricted region of the state space. How does this happen? One way to describe this bouncing is to plot the $(n+1)$ th intersection of the trajectory with the Poincaré surface as a function of the preceding intersection. Referring to figure 31.12 we find the map of figure 31.18. This is a Poincaré return map for the limit cycle. If we start at various points in the state space (keeping the non-linearity parameter fixed) and mark all passes as the trajectory converges to the limit cycle, we trace an approximately continuous curve $f(x)$ of figure 31.19 which gives the location of the trajectory at time $t + T_0$ as a function of its location at time t :

$$x_{n+1} = f(x_n). \tag{31.2}$$

The trajectory bounces within a trough in the state space, and $f(x)$ gives a local description of the way the trajectories converge to the limit cycle. In principle we know $f(x)$, as we can measure it, or compute it from the equations of motion. The form of $f(x)$ depends on the choice of Poincaré map, and an analytic expression for $f(x)$ is in general not available, but we know what $f(x)$ should look like; it has to fall on both sides (to confine the trajectory), so it has a maximum. Around the maximum it looks like a parabola

$$f(x) = a_0 + a_2(x - x_c)^2 + \dots \tag{31.3}$$

like any sensible polynomial approximation to a function with a hump.

This brings us to the problem of a rational approach to fishery. By means of a Poincaré map we have reduced a continuous trajectory in state space to 1-

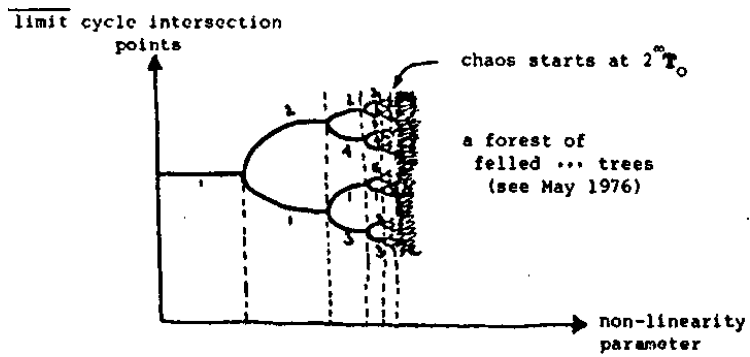


Figure 31.13:

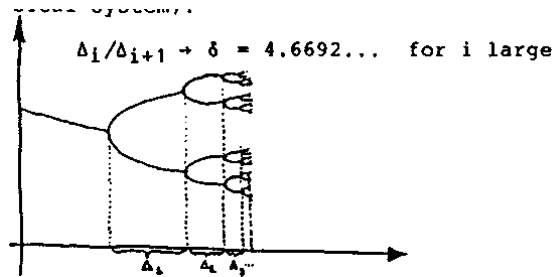


Figure 31.14:

dimensional iteration. This 1-dimensional iteration is studied in population biology, where $f(x)$ is interpreted as a population curve (the number of fish x_{n+1} in the given year as a function of the number of fish x_n the preceding year), and the bifurcation tree figure 31.13 has been studied in considerable detail.

The first thing we need to understand is the way in which a trajectory converges to a limit cycle. A numerical experiment will give us something like figure 31.21. In the Poincaré map the limit trajectory maps onto itself, $x_q = f(x_q)$. Hence a limit trajectory corresponds to a *fixed point* of $f(x)$. Take a programmable calculator and try to determine x_q . Type in a simple approximation to $f(x)$, such as

$$f(x) = \lambda - x^2. \tag{31.4}$$

Here λ is the non-linear parameter. Enter your guess x_0 and press the button. The number x_1 appears on the display. Is it a fixed point? Press the button again, and again, until $x_{n+1} = x_n$ to desired accuracy. Diagrammatically, this is illustrated by the web traced out by the trajectory in figure 31.22. Note the tremendous simplification gained by the use of the Poincaré map. Instead of computing the entire state space trajectory by a numerical integration of the equations of motion, we are merely pressing a button on the calculator.

This little calculation confirms one's intuition about fishery. Given a fishpond, and sufficient time, one expects the number of fish to stabilize. However, no such luck - a rational fishery manager soon discovers that anything can happen from year to year. The reason is that the fixed point x_q need not be attractive, and our calculator computation need not converge.

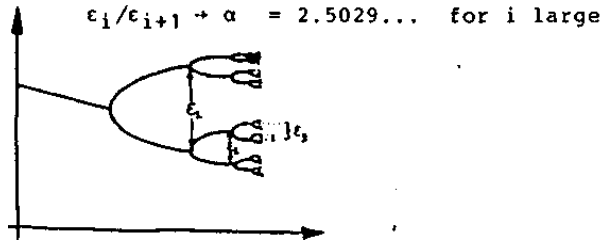
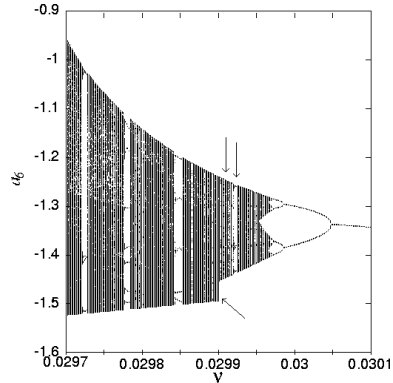


Figure 31.15:

Figure 31.16: A period-doubling tree observed in a small size Kuramoto-Sivashinsky system, generated under adiabatic change of the damping parameter (system size). The choice of projection down to the coordinate a_6 is arbitrary; projected down to any coordinate, the tree is qualitatively the same. The two upper arrows indicate typical values: for $\nu = 0.029910$ dynamics appears chaotic, and $\nu = 0.029924$ there is a ‘golden-mean’ repelling set coexisting with attractive period-3 window. The lower arrow indicates the value at which upper invariant set with this merges with its $u(x) \rightarrow -u(-x)$ symmetry partner. $N = 16$ Fourier modes truncation of (30.13). Truncation to $N = 17$ modes yields a similar figure, with values for specific bifurcation points shifted by $\sim 10^{-5}$ with respect to the $N = 16$ values. (from ref. [79])



31.4 A universal equation

Why is the naive fishery manager wrong in concluding that the number of fish will eventually stabilize? He is right when he says that $x_q = f(x_q)$ corresponds to the same number of fish every year. However, this is not necessarily a stable situation. Reconsider how we got to the fixed point in figure 31.22. Starting with a sufficiently good guess, the iterates converge to the fixed point. Now start increasing gently the non-linearity parameter (Rayleigh number, the nutritional value of the pond, etc.). $f(x)$ will slowly change shape, getting steeper and steeper at the fixed point, until the fixed point becomes unstable and gives birth to a cycle of two points. This is precisely the first bifurcation observed in our experiments.

Example 31.2 Fixed point stability.

The fixed point condition for map (31.4) $x^2 + x - \lambda = 0$ yields 2 fixed points.

$$x_{pm} = \frac{-1 \pm \sqrt{1 + 4\lambda}}{\text{what?}}$$

The fixed point x_+ loses stability at $\lambda = -1$. Inserted into $\lambda = f'(x) = -2x$, this yields

$$\lambda = 3/4, \quad x_+ = 1/2$$

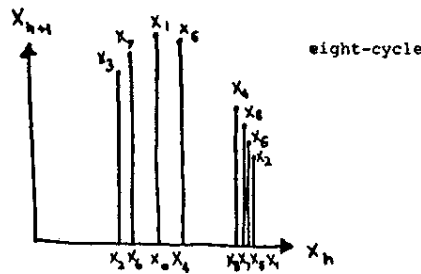
as the value at which fixed point x_+ loses stability.

This is the only gentle way in which our trajectory can become unstable (cycles of other lengths can be created, but that requires delicate fiddling with parameters; such bifurcations are not generic). Now we return to the same point after

Figure 31.17:



Figure 31.18:



every second iteration

$$x_i = f(f(x_i)), \quad i = 1, 2.$$

exercise 31.1

so the periodic points of $f(x)$ are the fixed points of $f(f(x))$.

To study their stability, we plot $f(f(x))$ alongside $f(x)$ in figure 31.24. What happens as we continue to increase the “Rayleigh number”? $f(x)$ becomes steeper at its fixed point, and so does $f(f(x))$. Eventually the magnitude of the slope at the fixed points of $f(f(x))$ exceeds one, and they bifurcate. Now the cycle is of length four, and we can study the stability of the fixed points of the fourth iterate. They too will bifurcate, and so forth. This is why the state space trajectories keep on splitting $2 \rightarrow 4 \rightarrow 8 \rightarrow 16 \rightarrow 32 \dots$ in our experiments. The argument does not depend on the precise form of $f(x)$, and therefore the phenomenon of successive period-doublings is *universal*.

More amazingly, this universality is not only qualitative. In our analysis of the stability of fixed points we kept on magnifying the neighborhood of the fixed point, figure 31.25. The neighborhoods of successive fixed points look very much the same after iteration and rescaling. After we have magnified the neighborhoods of fixed points many times, practically all information about the global shape of the starting function $f(x)$ is lost, and we are left with a *universal function* $g(x)$. Denote by T the operation indicated in figure 31.25 iterate twice and rescale by (without changing the non-linearity parameter),

$$Tf(x) = \alpha f(f(x/\alpha)), \tag{31.5}$$

$g(x)$ is self-replicating under rescaling and iteration, figure 31.26. More precisely, this can be stated as the *universal equation*

$$g(x) = \alpha g(g(-x/\alpha)), \tag{31.6}$$

which determines both the universal function $g(x)$ and $\alpha = -1/g(1) = 2.50290787\dots$, with normalization convention $g(0) = 1$.

Example 31.3 An approximate period doubling renormalization.

As the simplest examples of period-doubling cascades. Consider the map

$$x_{n+1} = f_\lambda(x_n) = \lambda - x_n^2, \quad \lambda, x \in \mathbb{R}. \tag{31.7}$$

Figure 31.19:

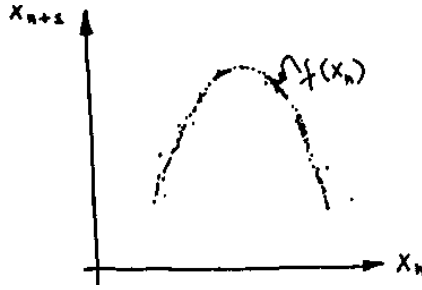
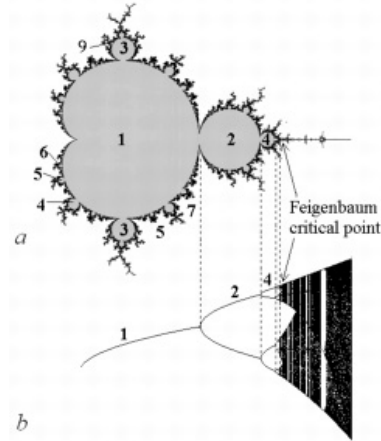


Figure 31.20: Correspondence between (a) the Mandelbrot set, shown in plane $(\text{Re}\lambda, \text{Im}\lambda)$ for the map $z_{k+1} = \lambda - z_k^2$, and (b) the period-doubling bifurcation tree, plane (λ, x) , $x, \lambda \in \mathbb{R}$. (from refs. [?, 31])



The two fixed points of f , $x_{\pm} = \frac{1 \pm \sqrt{1+4\lambda}}{2}$, are the roots of $x_* = \lambda - x_*^2$. At $\lambda = 3/4$ the Floquet multiplier $\Lambda = f'_{\lambda}(x_*)$ of the fixed point $x_* = \frac{1 + \sqrt{1+4\lambda}}{2}$ is marginal, $\Lambda = -2x_* = -1$. For $\lambda > 3/4$, the fixed point loses its stability and undergoes a period-doubling bifurcation. Values λ for subsequent bifurcations can be found by means of the following approximate renormalization method. Apply the map (31.7) two times:

$$x_{n+2} = \lambda - \lambda^2 + 2\lambda x_n^2 - x_n^4, \tag{31.8}$$

and drop the quartic term x_n^4 . By the scale transformation

$$x_n \rightarrow x_n/\alpha_0, \quad \alpha_0 = -2\lambda, \tag{31.9}$$

this can be rewritten in the original form $x_{n+2} = \lambda_1 - x_n^2$, which differs from (31.7) only by renormalization of λ

$$\lambda_1 = \varphi(\lambda) = -2\lambda(\lambda - \lambda^2). \tag{31.10}$$

The map parameterized by λ , approximates two applications of the original map. Repeating the renormalization transformation (31.10) with scale factors $\alpha_m = -2\lambda_m$, one obtains a sequence of the form

$$x_{n+2^m} = \lambda_m - x_n^2, \quad \lambda_m = \varphi(\lambda_{m-1}). \tag{31.11}$$

Fixed points of these maps correspond to the 2^m -cycles of the original map. All these cycles, as well as the fixed point of the map (31.7), become unstable at $\lambda_m = \Lambda_1 = 3/4$. Solving the chain of equations

$$\Lambda_1 = \varphi(\Lambda_2) \Lambda_2 = \varphi(\Lambda_3) \dots \Lambda_{m-1} = \varphi(\Lambda_m), \tag{31.12}$$

we get the corresponding sequence of bifurcation values of parameter λ (with $\lambda \approx \Lambda_m$ the 2^m -cycle of (31.7)). From iteration diagram of figure 31.27 it is evident, that

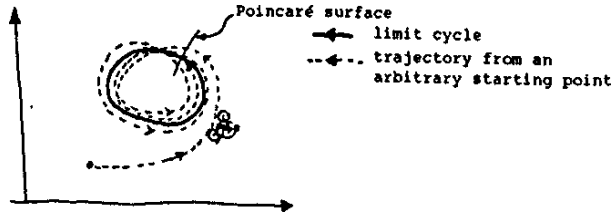


Figure 31.21:

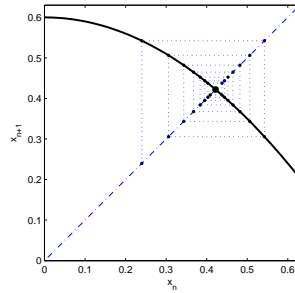


Figure 31.22:

this sequence converges with $m \rightarrow \infty$ to a definite limit Λ_∞ , the fixed point of the renormalization transformation. It satisfies the equation $\Lambda_\infty = \varphi(\Lambda_\infty)$, thus $\Lambda_\infty = (1 + \sqrt{3})/2 \approx 1.37$. The scaling factors also converge to the limit: $\alpha_m \rightarrow \alpha$, where $\alpha = -2\Lambda_\infty \approx 2.74$. The multipliers (Floquet multipliers of the 2^m -cycles) converge to $\mu_m \rightarrow \mu = \sqrt{1 - 4\Lambda_\infty} \approx -1.54$.

From transformation (31.11) one can also describe the convergence of the bifurcation sequence:

$$\begin{aligned} \Lambda_m &= \varphi(\Lambda_\infty) + \varphi'(\Lambda_\infty)(\Lambda_{m+1} - \Lambda_\infty) = \\ &= \Lambda_\infty + \delta(\Lambda_{m+1} - \Lambda_\infty) \end{aligned} \quad (31.13)$$

where the Feigenbaum $\delta = \varphi'(\Lambda_\infty) = 4 + \sqrt{3} \approx 5.73$ characterizes parameter rescaling for each successive period doubling.

The approximate values of Feigenbaum's universal space and parameter scaling constants are reasonably close to the exact values,

	exact	approximate	
α	=	$-2.502 \dots$	-2.74
δ	=	$4.669 \dots$	5.73 ,

considering the crudeness of the approximation: the universal fixed-point function $g(x)$ is here truncated to a quadratic polynomial.

(O.B. Isaeva and S.P. Kuznetsov)

If you arrive at $g(x)$ the way we have, by successive bifurcations and rescaling, you can hardly doubt its existence. However, if you start with (31.6) as an equation to solve, it is not obvious what its solutions should look like. The simplest thing to do is to approximate $g(x)$ by a finite polynomial and solve the universal equation numerically, by Newton method. This way you can compute α and δ to much higher accuracy than you can ever hope to measure them experimentally.

There is much pretty mathematics in universality theory. Despite its simplicity, nobody seems to have written down the universal equation before 1976, so

Figure 31.23:

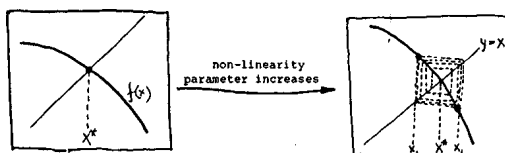
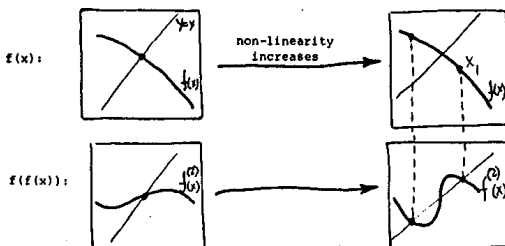


Figure 31.24:



the subject is still young. We do not have a series expansion for α , or an analytic expression for $g(x)$; the numbers that we have are obtained by boring numerical methods. So far, all we know is that $g(x)$ exists. What has been proved is that the Newton iteration converges, so we are no wiser for the result.

To see why the universal function must be a rather crazy function, consider high iterates of $f(x)$ for parameter values corresponding to 2-, 4- and 8-cycles, figure 31.28. If you start anywhere in the unit interval and iterate a very large number of times, you end up in one of the periodic points. For the 2-cycle there are two possible limit values, so $f(f(\dots f(x)))$ resembles a castle battlement. Note the infinitely many intervals accumulating at the unstable $x = 0$ fixed point. In a bifurcation of the 2-cycle into the 4-cycle each of these intervals gets replaced by a smaller battlement. After infinitely many bifurcations this becomes a fractal (i.e., looks the same under any enlargement), with battlements within battlements on every scale. Our universal function $g(x)$ does not look like that close to the origin, because we have enlarged that region by the factor $\alpha = 2.5029\dots$ after each period-doubling, but all the wiggles are still there; you can see them in Feigenbaum's (1978) plot of $g(x)$. For example, (31.6) implies that if x_q is a fixed point of $g(x)$, so is $\alpha(x_q)$. Hence $g(x)$ must cross the lines $y = x$ and $y = -x$ infinitely many times. It is clear that while around the origin $g(x)$ is roughly a parabola and well approximated by a finite polynomial, something more clever is needed to describe the infinity of $g(x)$'s wiggles further along the real axis and in the complex plane.

All this is fun, but not essential for understanding the physics of the onset of chaos. The main thing is that we now understand where the universality comes from. We start with a complicated many-dimensional dynamical system. A Poincaré map reduces the problem from a study of differential equations to a study of discrete iterations, and dissipation reduces this further to a study of 1-dimensional iterations (now we finally understand why the state space trajectory in the turbulence experiment undergoes a series of bifurcations as we turn the heat up!). The successive bifurcations take place in smaller and smaller regions of the state space. After n bifurcations the trajectory splittings are of order $\alpha^{-n} = (0.399\dots)^{-n}$ and practically all memory of the global structure of the original dynamical system is lost (see figure 31.29). The asymptotic self-similarities can be encoded by

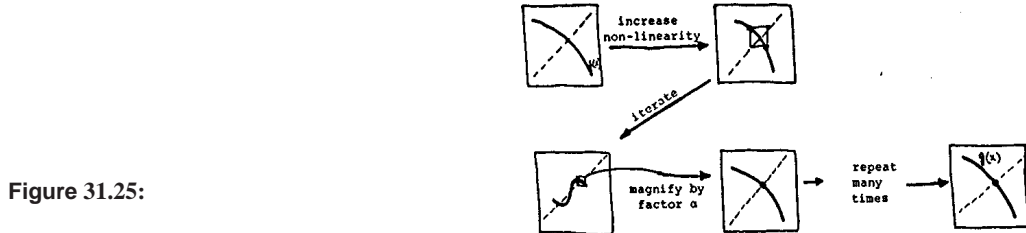


Figure 31.25:

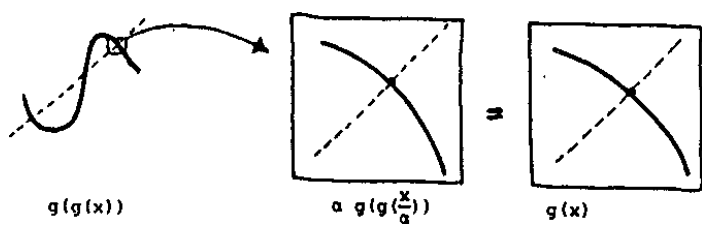


Figure 31.26:

universal equations. The physically interesting scaling numbers can be quickly estimated by simple truncations of the universal equations, such as example 31.3. The full universal equations are designed for accurate determinations of universal numbers; as they have built-in rescaling, the round-off errors do not accumulate, and the only limit on the precision of the calculation is the machine precision of the computer.

Anything that can be extracted from the asymptotic period-doubling regime is universal; the trick is to identify those universal features that have a chance of being experimentally measurable. We will discuss several such extensions of the universality theory in the remainder of this introduction.

31.5 The unstable manifold

Feigenbaum delta

$$\begin{aligned} \delta &= \lim_{n \rightarrow \infty} \frac{r_{n-1} - r_n}{r_n - r_{n+1}} \\ &= 4.6692016\dots \end{aligned} \tag{31.14}$$

is the universal number of the most immediate experimental import - it tells us that in order to reach the next bifurcation we should increase the Rayleigh number (or friction, or whatever the controllable parameter is in the given experiment) by about one fifth of the preceding increment. Which particular parameter is being varied is largely a question of experimental expedience; if r is replaced by another parameter $R = R(r)$, then the Taylor expansion

$$R(r) = R(r_\infty) + (r - r_\infty)R'(r_\infty) + (r - r_\infty)^2 R''(r_\infty)/2 + \dots$$

yields the same asymptotic delta

$$\delta \simeq \frac{R(r_{n-1}) - R(r_n)}{R(r_n) - R(r_{n+1})} = \frac{r_{n-1} - r_n}{r_n - r_{n+1}} + O(\delta^n) \tag{31.15}$$

exercise 31.3

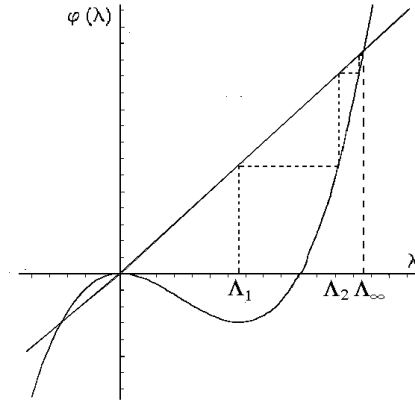


Figure 31.27: Iteration of the approximate renormalization transformation (31.10). Dashed line designates the backward iterations starting at the first period doubling bifurcation point, $\lambda_1 = 3/4$, and mapping to the further bifurcation points λ_m .

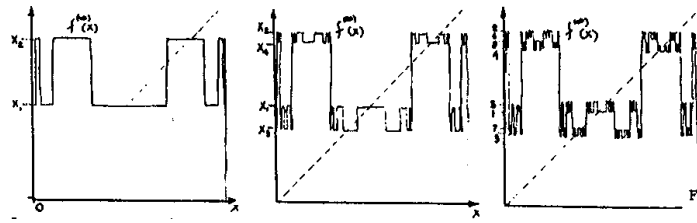


Figure 31.28:

providing, of course, that $R'(r_\infty)$ is non-vanishing (the chance that a physical system just happens to be parameterized in such a way that $R(r_\infty) = 0$ is nil).

In deriving the universal equation (31.6) we were intentionally sloppy, because we wanted to introduce the notion of encoding self-similarity by universal equations without getting entangled in too much detail. We obtained a universal equation which describes the self-similarity in the x -space, under iteration and rescaling by α . However, the bifurcation tree figure 31.13 is self-similar both in the x -space and the parameter space: each branch looks like the entire bifurcation tree. We will exploit this fact to construct a universal equation which determines both α and δ .

Let T^* denote the operation of iterating twice, rescaling x by α , *shifting* the non-linearity parameter to the corresponding value at the next bifurcation (more precisely, the value of the nonlinearity parameter with the same *stability*, i.e., the same slope at the periodic points), and *rescaling* it by δ :

$$T^* f_{R_n + \Delta_n p}(x) = \alpha_n f_{R_n + \Delta_n(1+p/\delta_n)}^{(2)}(x/\alpha_n) \tag{31.16}$$

Here R_n is a value of the non-linearity parameter for which the limit cycle is of length 2^n , Δ_n is the distance to R_{n+1} , $\delta_n = \Delta_n/\Delta_{n+1}$, p provides a continuous parametrization, and we apologize that there are so many subscripts. T^* operation encodes the self-similarity of the bifurcation tree figure 31.13, see figure 31.30.

For example, if we take the fish population curve $f(x)$, Eq. (31.4), with R value corresponding to a cycle of length 2^n , and act with T^* , the result will be a similar cycle of length 2^n , but on a scale α times smaller. If we apply T^* infinitely many times, the result will be a universal function with a cycle of length 2^n :

$$g_p(x) = (T^*)^\infty f_{R+p\Delta}(x) \tag{31.17}$$

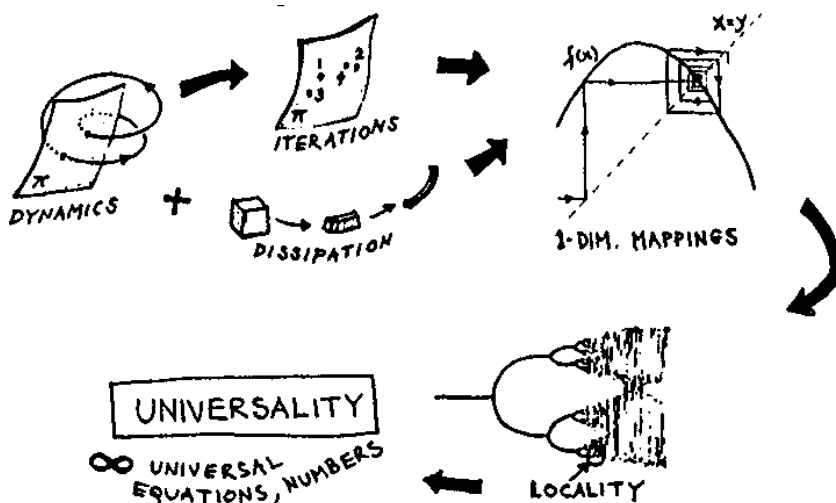


Figure 31.29:

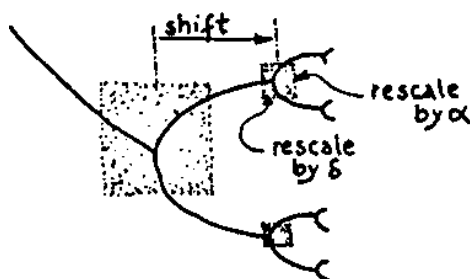


Figure 31.30:

If you can visualize a space of all functions with quadratic maximum, you will find figure 31.31 helpful. Each transverse sheet is a manifold consisting of functions with 2^n -cycle of given stability. T^* moves us across this transverse manifold toward g_p .

$g_p(x)$ is invariant under the self-similarity operation T^* , so it satisfies a universal equation

$$g_p(x) = \alpha g_{1+p/\delta}(g_{1+p/\delta}(x/\alpha)) \tag{31.18}$$

p parameterizes a 1-dimensional continuum family of universal functions. Our first universal equation (31.6) is the fixed point of the above equation:

$$p^* = 1 + p^*/\delta \tag{31.19}$$

and corresponds to the asymptotic 2^∞ -cycle.

The family of universal functions parameterized by p is called the *unstable manifold* because T -operation (31.5) drives p away from the fixed point value $g(x) = g_{p^*}(x)$.

You have probably forgotten by now, but we started this section promising a computation of δ . This we do by linearizing the equations (31.18) around the fixed point p^* . Close to the fixed point $g_p(x)$ does not differ much from $g(x)$, so one can treat it as a small deviation from $g(x)$:

$$g_p(x) = g(x) + (p - p^*)h(x)$$

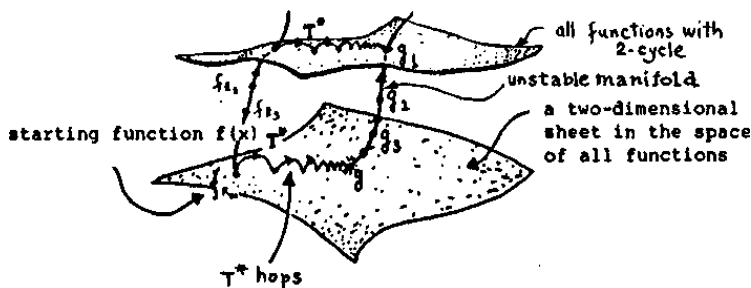


Figure 31.31:

Substitute this into (31.18), keep the leading term in $p - p^*$, and use the universal equation (31.6). This yields a universal equation for δ :

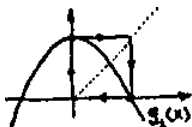
$$g'(g(x))h(x) + h(g(x)) = (\delta/\alpha)h(x) \tag{31.20}$$


We already know $g(x)$ and α , so this can be solved numerically by polynomial approximations, yielding $\delta = 4.6692016\dots$, together with a part of the spectrum of eigenvalues and eigenvectors $h(x)$.

Actually, one can do better with less work; T^* -operation treats the coordinate x and the parameter p on the same footing, which suggests that we should approximate the entire unstable manifold by a double power series

$$g_p(x) = \sum_{j=0}^N \sum_{k=0}^N c_{jk} x^{2j} p^k \tag{31.21}$$

The scale of x and p is arbitrary. We will fix it by the normalization conditions

$$g_0(0) = 0, \tag{31.22}$$


$$\begin{aligned} g_1(0) &= 1 \\ g_1(1) &= 0, \end{aligned} \tag{31.23}$$


The first condition means that the origin of p corresponds to the superstable fixed point. The second condition sets the scale of x and p by the superstable 2-cycle. (Superstable cycles are the cycles which have the maximum of the map as one of the periodic points.) Start with any simple approximation to $g_p(x)$ which satisfies the above conditions (for example, $g(x) = p - x^2$). Apply the T^* -operation (31.16) to it. This involves polynomial expansions in which terms of order higher than M and N in (31.21) are dropped. Now find by Newton method the value of δ which satisfies normalization (31.23). This is the only numerical calculation you have to do; the condition (31.23) automatically yields the value of α . The result is a new approximation to g_p . Keep applying T^* until the coefficients in (31.21) repeat; this has moved the approximate g_p toward the unstable manifold along the transverse sheets indicated in figure 31.31. Computationally this is straightforward, the accuracy of the computation is limited only by computer precision, and at the end you will have α , δ and a polynomial approximation to the unstable manifold $g_p(x)$.

As δ controls the convergence of the high iterates of the initial mapping toward their universal limit $g(x)$, it also controls the convergence of most other numbers toward their universal limits, such as the scaling number $\alpha_n = \alpha + O(\delta^{-n})$, or even δ itself, $\delta_n = \delta + O(\delta^{-n})$. As $1/\delta = 0.2141\dots$, the convergence is very rapid, and already after a few bifurcations the universality theory is good to a few per cent. This rapid convergence is both a blessing and a curse. It is a theorist's blessing because the asymptotic theory applies already after a few bifurcations; but it is an experimentalist's curse because a measurement of every successive bifurcation requires a fivefold increase in the experimental accuracy of the determination of the non-linearity parameter r .

Commentary

Remark 31.1 A brief history of period doubling universality. Mitchell J. Feigenbaum discovered universality in one-dimensional iterative maps in August 1975. Following Feigenbaum's functional formulation of the problem, in March 1976 Cvitanović derived collaboration with M.J. the equation (31.6) for the period doubling fixed point function (not a big step, it is the limit of Feigenbaum functional recursion sequence), which has since played a key role in the theory of transitions to turbulence. The first published report on Feigenbaum's discovery is dated August 1976 (Los Alamos Theoretical Division Annual Report 1975-1976, pp. 98-102, [read it here](#)). By that time the work had become widely known through many seminars Feigenbaum gave in US and Europe. His first paper, submitted to *Advances in Mathematics* in Nov 1976 was rejected. The second paper was submitted to *SIAM Journal of Applied Mathematics* in April 1977 and rejected in October 1977. Finally, J. Lebowitz published both papers [1, 2] without further referee pain (M. J. Feigenbaum, *J. Stat. Phys.* 19, 25 (1978) and 21, 6 (1979)).

A very informative review by May [3] describes what was known before Feigenbaum's contribution. The geometric parameter convergence was first noted by Myrberg (1958), and independently of Feigenbaum, by Grossmann and Thomae [4] (without noting the universality of δ). The theory of period-doubling universal equations and scaling functions is developed in Kenway's notes of Feigenbaum 1984 Edinburgh lectures [5] (trifle hard to track down). The elegant unstable manifold formulation of universality given in *ChaosBook.org* is due to Vul, Khanin, Sinai and Gol'dberg [?, 9, 4] in 1982. The most thorough exposition available is the Collet and Eckmann [6] monograph. By 1978 Couillet and Tresser [7, 8] have proposed similar equations. Daido (1981a) has introduced a different set of universal equations. Derrida, Gervois and Pomeau (1979) have extracted a great many metric universalities from the asymptotic regime. Grassberger (1981) has computed the Hausdorff dimension of the asymptotic attractor. Lorenz (1980) and Daido (1981b) have found a universal ratio relating bifurcations and reverse bifurcations. If $f(x)$ is not quadratic around the maximum, the universal numbers will be different - see Villela Mendés (1981) and Hu and Mao (1982b) for their values. According to Kuramoto and Koga (1982) such mappings can arise in chemical turbulence. Nonlinear oscillator; quadratic potential with damping and harmonic driving force exhibit cascades of period-doubling bifurcations [10, 11]. Refs. [12, 13, 14] compute solutions of the period-doubling fixed point equation using methods of Schöder and Abel, yielding what are so far the most accurate δ and α . See also ref. [15].

Since then we have generalized the universal equations to period n -tuplings; constructed universal scaling functions for all winding numbers in circle maps, and established universality of the Hausdorff dimension of the critical staircase. A nice discussion

of circle maps and their physical applications is given in refs. [17, 4, 5]. The universality theory for golden mean scalings is developed in refs. [12, 8, 10, 11]. The scaling functions for circle maps are discussed in ref. [13].

The theory would have remained a curiosity, were it not for the beautiful experiment by Libchaber and Maurer (1981), and many others that followed. Crucial insights came from Collet and Eckmann (1980a) and Collet, Eckmann and Koch (1980) who explained how the dynamics of dissipative system (such as a viscous fluid) can become becomes 1-dimensional. The experimental and theoretical developments up to 1990's are summarized in reprint collections by P. Cvitanović [5] and B.-L. Hao [26]. We also recommend Hu (1982), Crutchfield, Farmer and Huberman (1982), Eckmann (1981) and Ott (1981). The period-doubling route to turbulence that is by no means the only way to get there; see Eckmann (1981) discussion of other routes to chaos.

By 1979 mathematicians also understood that the numerical methods used by Feigenbaum and Cvitanović to solve the universal equations were in fact convergent. Mathematicians did what they do; they attached various names to the equations, and they changed letters around to make the equations unintelligible to physicists. The re-lettering did not stick, but the renamings did. (This chapter is based on a Nordita lecture prepared together with Mogens Høgh Jensen (Cvitanović and Høgh Jensen 1982). Ulla Selmer prepared the drawings, Oblivia Kaypro stood for the initial execution.)

Exercises

- 31.1. **Period doubling in your pocket:** Take a programmable pocket calculator or Matlab or whatever makes you feel good and program the function

$$f(x) = \lambda - x^2.$$

The game consists in staring at the display, and looking for regularities in the sequences of iterates.

- (a) (no thinking) Try to determine fixed point x_* = $f(x_*)$ by blind iteration. Chose some value of λ a bit bigger than 0, and initial x between -1 and 1. Enter the initial x_0 and read off the next x_1 . Start again, with x_1 as input. The number x_2 appears on the display. Is it a fixed point? Press the button again, and again, until $x_n = x_*$ to desired accuracy.
- (f) (no thinking) Increase λ in small steps, as long as the trajectory does not blow up, let transients die, and then plot few hundred consecutive x_n . Generate a figure to replace the hand drawn figure 31.14.
- (c) (thinking) Determine the smallest positive λ for which almost any initial x_0 iterates to $-\infty$.

- (b) (no thinking) Try $\lambda = 3/4$. How's the convergence now?
- (c) (thinking) Determine λ for which the fixed point x_* goes unstable.
- (d) (no thinking) Try also λ : 1, 1.31070274134, 1.38154748443, 1.3979453597.
- (e) (thinking) Compute the next number in this series. Estimate Feigenbaum δ .
- (g) (thinking) Determine numerically scaling factors α_m which overlay (approximately) neighborhood of $x = 0$ for superstable $f^{2^{m-1}}(x)$ over the neighborhood for $\alpha_m f^{2^m}(f^{2^m}(x/\alpha_m))$ for 4, 8, 16, \dots superstable cycles. Draw a figure to replace the hand drawn figure 31.26.

(P. Cvitanović)

- 31.2. **Period doubling in a 3-dimensional flow:** This is a more time consuming problem, but it gives you a feel for how numerical experiments in nonlinear dynamics are *really* done, and sets you up for doing real-life problems later on.

Consider the nonlinear oscillator

$$\frac{d^2}{dt^2}x + k\frac{d}{dt}x - x + 4x^3 = A \cos(\omega t). \quad (31.24)$$

The oscillator is driven by an external force of frequency ω , with amplitude A and the natural time unit $T_0 = 2\pi/\omega$. The dissipation is controlled by the friction coefficient k .

Given the initial displacement and velocity one can easily follow numerically (by the Runge-Kutta method, for example) the state space trajectories of the system. Due to the dissipation it does not matter where one starts in the state space. For a strong friction or a weak forcing a wide range of initial points converge to a fixed point or a limit cycle (trajectory loops onto itself). However, as one decreases the friction, bifurcations and chaos are observed.

- Rewrite as a nonautonomous system of 2 first order ODEs.
- Rewrite as an autonomous system of 3 first order ODEs (add an equation whose solution is $\cos(\omega t)$).
- Observe long-time trajectories for $k = 0.154$, $\omega = 1.2199778$ and A in some range like $A = 0.05$ to 0.2 . Anything interesting happening? [Helpful tips: let the system run for sufficiently long time that the transients have had time to die out. Whenever changing the parameter (in this case, parameter A), increase parameter in small steps (adiabatically), and then restart the trajectory from the last point of the preceding simulation. This minimizes the transients.]
- Construct a stroboscopic Poincaré section by recording values of (x_n, \dot{x}_n) at times separated $T_0, 2T_0, \dots, 2^n T_0, \dots$

- Play a bit with plotting various combinations of x_n, x_{n+1}, \dot{x}_n , and \dot{x}_{n+1} . Often a Poincaré return map - such as (x_n, x_{n+1}) - is more informative than a Poincaré section, such as (x_n, \dot{x}_n) .
- Increase A in small steps, as long as the trajectory does not blow up, let transients die, and then plot a few hundred consecutive x_n (or whatever variable you like best). Plot a (A, x_n) period-doubling tree to replace the hand drawn figure 31.14.
- Observe long-time trajectories for $(k, \omega) = (0.154, 1.2199778)$ and $A = 0.1, 0.11, 0.114, 0.11437, \dots$. Do you observe bifurcations?

There is nothing special about these parameter values; we give them just to help you with finding your first bifurcation sequence in a realistic nonlinear flow.

(P. Cvitanović)

31.3. Renormalization in a 3-dimensional flow:



Consider the nonlinear oscillator (31.24).

- For $(k, \omega) = (0.154, 1.2199778)$ determine accurately amplitude values $A_1, A_2, \dots, A_n, \dots$, for which 2^n -cycle bifurcates into 2^{n+1} -cycle. [Tip: use the Newton method on the Poincaré section. You'll need to also integrate the linearized stability matrix.]
- Estimate Feigenbaum δ .
- Estimate Feigenbaum α .

(P. Cvitanović)

References

- [31.1] M. J. Feigenbaum, Quantitative universality for a class of nonlinear transformations, *J. Stat. Phys.* **19**, 25 (1978).
- [31.2] M. J. Feigenbaum, The universal metric properties of nonlinear transformations, *J. Stat. Phys.* **21**, 669 (1979), Reprinted in ref. [5].
- [31.3] R. May, Simple mathematical models with very complicated dynamics, *Nature* **261**, 459 (1976).
- [31.4] S. Grossmann and S. Thomae, Invariant distributions and stationary correlation functions of one-dimensional discrete processes, *Z. Naturforsch. A* **32**, 1353 (1977).

- [31.5] M. J. Feigenbaum and R. D. Kenway, The onset of chaos, in *Statistical and Particle Physics*, edited by K. C. Bowler and A. J. McKane, pp. 1–100, Edinburgh, 1983, Proc. 26th Scottish Universities Summer School in Physics, SUSSP Publ.
- [31.6] P. Collet and J.-P. Eckmann, *Iterated Maps on the Interval as Dynamical Systems* (Birkhäuser, Boston, 1980).
- [31.7] P. Coullet and C. Tresser, Itérations d’endomorphismes et groupe de renormalisation, *J. de Physique Colloque C* **39**, 5 (1978).
- [31.8] P. Coullet and C. Tresser, Itérations d’endomorphismes et groupe de renormalisation, *C. R. Acad. Sci. Paris A* **287**, 577 (1978).
- [31.9] A. J. Dragt, Lie methods for nonlinear dynamics with applications to accelerator physics, www.physics.umd.edu/dsat/dsatliemethods.html, 2011.
- [31.10] F. C. Moon, *Chaotic Vibrations: An Introduction for Applied Scientists and Engineers* (Wiley, New York, 1987).
- [31.11] A. Y. Kuznetsova, A. P. Kuznetsov, C. Knudsen, and E. Mosekilde, Catastrophe theoretic classification of nonlinear oscillators, *Int. J. Bif. Chaos* **14**, 1241 (2004).
- [31.12] K. Briggs, A precise calculation of the Feigenbaum constants, *Mathematics of Computation* **57**, 435 (1991).
- [31.13] K. M. Briggs, G. R. W. Quispel, and C. J. Thompson, Feigenvalues for Mandelsets, *J. Phys. A* **24**, 3363 (1991).
- [31.14] K. M. Briggs, T. W. Dixon, and G. Szekeres, *Analytic solutions of the Cvitanović-Feigenbaum and Feigenbaum-Kadanoff-Shenker equations*, *Int. J. Bif. Chaos* **8**, 347 (1998).
- [31.15] E. W. Weisstein, Feigenbaum constant, 2012, mathworld.wolfram.com/FeigenbaumConstant.html.
- [31.16] “Feigenbaum Function,” mathworld.wolfram.com/FeigenbaumFunction.html.
- [31.17] M. H. Jensen, P. Bak, and T. Bohr, Complete devil’s staircase fractal dimension and universality of mode-locking structure in the circle map, *Phys. Rev. Lett.* **50**, 1637 (1983).
- [31.18] M. H. Jensen, P. Bak, and T. Bohr, Transition to chaos by interaction of resonances in dissipative systems. I. Circle maps, *Phys. Rev. A* **30**, 1960 (1984).
- [31.19] P. Bak, T. Bohr, and M. H. Jensen, Mode-locking and the transition to chaos in dissipative systems, *Phys. Scr.* **T9**, 50 (1985).
- [31.20] S. Shenker, Scaling behavior in a map of a circle onto itself: Empirical results, *Physica D* **5**, 405 (1982).

- [31.21] M. Feigenbaum, L. Kadanoff, and S. Shenker, Quasiperiodicity in dissipative systems: A renormalization group analysis, *Physica D* **5**, 370 (1982).
- [31.22] D. Rand, S. Ostlund, J. Sethna, and E. Siggia, Universal transition from quasiperiodicity to chaos in dissipative systems, *Phys. Rev. Lett.* **49**, 132 (1982).
- [31.23] J. Sethna, S. Ostlund, D. A. Rand, and E. Siggia, Universal properties of the transition from quasi-periodicity to chaos in dissipative systems, *Physica D* **8**, 303 (1983).
- [31.24] J. Stavans, F. Heslot, and A. Libchaber, Fixed winding number and the quasiperiodic route to chaos in a convective fluid. *Phys. Rev. Lett.* **55**, 1239 (1985).
- [31.25] P. Cvitanović, B. Shraiman, and B. Söderberg, Scaling laws for mode lockings in circle maps, *Phys. Scr.* **32**, 263 (1985).
- [31.26] B.-L. Hao, *Chaos II* (World Scientific, Singapore, 1990).
- [31.27] M. Pollicott, “A Note on the Artuso-Aurell-Cvitanović approach to the Feigenbaum tangent operator,” *J. Stat. Phys.*, **62**, 257 (1991).
- [31.28] Y. Jiang, T. Morita and D. Sullivan, “Expanding direction of the period doubling operator,” *Comm. Math. Phys.* **144**, 509 (1992).
- [31.29] S.P. Kuznetsov and A.H. Osbaldestin, “Generalized dimensions of Feigenbaum’s attractor from renormalization-group functional equations,” [arXiv:nlin.CD/0204059](https://arxiv.org/abs/nlin.CD/0204059).
- [31.30] Tsygvintsev A.V.; Mestel B.D.; Osbaldestin A.H., “Continued fractions and solutions of the Feigenbaum-Cvitanović equation,” *Comptes Rendus Math.* **334**, 683 (2002).
- [31.31] O.B. Isaeva and S.P. Kuznetsov, “Approximate description of the Mandelbrot Set. Thermodynamic analogy,” [arXiv:nlin.CD/0504063](https://arxiv.org/abs/nlin.CD/0504063). *Nonlinear Phenomena in Complex Systems* **8**, 157 (2005).